AAV-Mediated CRISPR/Cas Gene Editing of Retinal Cells In Vivo

Sandy S. C. Hung,[1] Vicki Chrysostomou,[1] Fan Li,[1,2] Jeremiah K. H. Lim,[3] Jiang-Hui Wang,[1] Joseph E. Powell,[4,5] Leilei Tu,[1,6] Maciej Daniszewski,[1] Camden Lo,[7] Raymond C. Wong,[1] Jonathan G. Crowston,[1] Alice Pébay,[1] Anna E. King,[8] Bang V. Bui,[3] Guei-Sheung Liu,[1] and Alex W. Hewitt[1,2]

[1]Centre for Eye Research Australia, University of Melbourne, Royal Victorian Eye and Ear Hospital, Melbourne, Victoria, Australia
[2]Menzies Institute for Medical Research, School of Medicine, University of Tasmania, Hobart, Tasmania, Australia
[3]Department of Optometry & Vision Sciences, University of Melbourne, Melbourne, Victoria, Australia
[4]Institute for Molecular Bioscience, University of Queensland, Brisbane, Queensland, Australia
[5]Centre for Neurogenetics and Statistical Genomics, Queensland Brain Institute, University of Queensland, Brisbane, Queensland, Australia
[6]Department of Ophthalmology, Jinan University, Guangzhou, Guangdong, China
[7]Monash Micro Imaging, Monash University, Melbourne, Victoria, Australia
[8]Wicking Dementia Research and Education Centre, University of Tasmania, Hobart, Tasmania, Australia

Correspondence: Alex W. Hewitt, Menzies Institute for Medical Research, University of Tasmania, Hobart, 7000; Australia; hewitt.alex@gmail.com.

SSCH, G-SL, and AWH contributed equally to the work presented here and should therefore be regarded as equivalent authors.

Submitted: February 10, 2016
Accepted: May 25, 2016

Citation: Hung SSC, Chrysostomou V, Li F, et al. AAV-mediated CRISPR/Cas gene editing of retinal cells in vivo. *Invest Ophthalmol Vis Sci.* 2016;57:3470–3476. DOI:10.1167/iovs.16-19316

Purpose. Clustered Regularly Interspaced Short Palindromic Repeats (CRISPR)/CRISPR-associated protein (Cas) has recently been adapted to enable efficient editing of the mammalian genome, opening novel avenues for therapeutic intervention of inherited diseases. In seeking to disrupt yellow fluorescent protein (YFP) in a Thy1-YFP transgenic mouse, we assessed the feasibility of utilizing the adeno-associated virus 2 (AAV2) to deliver CRISPR/Cas for gene modification of retinal cells in vivo.

Methods. Single guide RNA (sgRNA) plasmids were designed to target *YFP*, and after in vitro validation, selected guides were cloned into a dual AAV system. One AAV2 construct was used to deliver *Streptococcus pyogenes* Cas9 (SpCas9), and the other delivered sgRNA against *YFP* or *LacZ* (control) in the presence of mCherry. Five weeks after intravitreal injection, retinal function was determined using electroretinography, and CRISPR/Cas-mediated gene modifications were quantified in retinal flat mounts.

Results. Adeno-associated virus 2–mediated in vivo delivery of SpCas9 with sgRNA targeting *YFP* significantly reduced the number of YFP fluorescent cells of the inner retina of our transgenic mouse model. Overall, we found an 84.0% (95% confidence interval [CI]: 81.8–86.9) reduction of YFP-positive cells in *YFP*-sgRNA–infected retinal cells compared to eyes treated with *LacZ*-sgRNA. Electroretinography profiling found no significant alteration in retinal function following AAV2-mediated delivery of CRISPR/Cas components compared to contralateral untreated eyes.

Conclusions. Thy1-YFP transgenic mice were used as a rapid quantifiable means to assess the efficacy of CRISPR/Cas-based retinal gene modification in vivo. We demonstrate that genomic modification of cells in the adult retina can be readily achieved by viral-mediated delivery of CRISPR/Cas.

Keywords: Cas9, guide RNA, CRISPR, in vivo, gene editing

Many ophthalmic diseases manifest due to well-defined genetic mutations, and inherited retinal diseases now compose the leading cause of blind registrations in working-aged individuals.[1] Inherited retinal dystrophies are a very heterogeneous group of conditions, all of which are as yet currently untreatable.[2,3] For example, over 100 disease-causing variants across 21 loci have been found to cause Leber congenital amaurosis (LCA).[4] To date, much work with LCA has focused on viral-mediated gene replacement therapy, where gene expression is augmented by ectopic replacement of a normal gene product.[5] However, emerging data for LCA2 suggest that the efficacy of such viral-mediated gene replacement therapy may decrease over time.[6,7] Additionally, genetic heterogeneity and restrictions in viral payloads limit the broad application of such an approach for many inherited retinal diseases.[8–10]

The Clustered Regularly Interspaced Short Palindromic Repeats (CRISPR) and CRISPR-associated protein (Cas) system used by bacteria to counter viral intrusion has recently been adapted to allow efficient editing of the mammalian nuclear genome.[11,12] CRISPR/Cas-based technology is particularly attractive for treating inherited diseases caused by genes with very specific spatial and stoichiometric expression.[5]

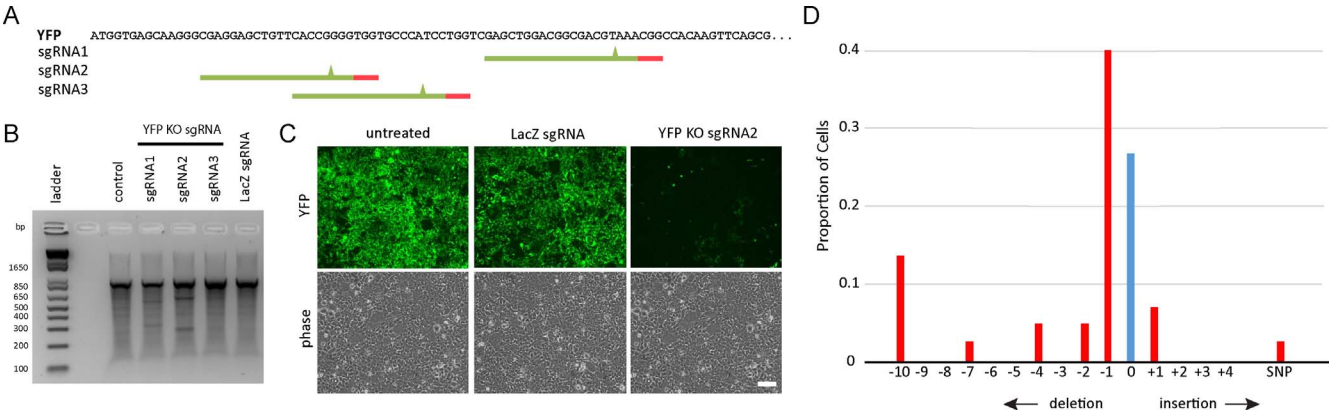

Figure 1. sgRNA design, plasmid construction, and validation for knockout (KO) of yellow fluorescent protein (YFP). (**A**) YFP target sequence used for sgRNA design. Selected sgRNA ideograms display the PAM sequence (*red*) and putative cut site (*green triangle*). Indel analysis using a SURVEYOR assay identified YFP KO sgRNA2 as having the best KO efficiency in our 3T3-L1-YFP line (**B**), and this was confirmed in vitro using the HEK293A-YFP line (**C**). *Scale bar*: 100 μm. Spectrum and frequency of indels induced by YFP-sgRNA for knockout of yellow fluorescent protein (YFP) in our 3T3-L1-YFP cell line were determined using TOPO TA cloning (**D**). One clone was found to have a single nucleotide substitution (SNP) at the predicted cut site, but no associated indel. $n = 45$ clones.

There have been a small number of studies, which have demonstrated the potential of in vivo gene editing for therapeutic applications.[13] Although the first reported in vivo application of CRISPR/Cas used the endogenous homology-directed repair pathway to correct the precise disease-causing mutation,[14] the majority of subsequent reports have used CRISPR/Cas for gene knockout.[15–17] In postmitotic cells, such as those found in the adult retina, double-stranded DNA breaks are preferentially repaired through nonhomologous end joining, and as such, diseases caused by gain of function, dominant negative, or increased copy number variants could be readily amenable to preemptive intervention whereby CRISPR/Cas technology is used to disrupt the mutant allele.

CRISPR/Cas gene editing has been applied to the retina in vivo using electroporation.[18,19] Wang and colleagues[18] electroporated constructs expressing *Streptococcus pyogenes* Cas9 (SpCas9) to disrupt the function of *Blimp1* and thereby dissect the molecular pathways involved in the regulation of murine retinal rod and bipolar cell development in vivo. More recently, Bakondi et al.[19] reported the use of electroporation to transfect photoreceptors with a plasmid containing SpCas9 and a single guide RNA (sgRNA) targeting the *Rho* gene in rats harboring the dominant *Rho* S334ter mutation. Strikingly, this intervention was found to prevent retinal degeneration and improve visual function.[19] Nonetheless, despite these promising applications, it is clear that such approaches for CRISPR/Cas delivery in vivo are not currently applicable as a human therapy.

The aim of our work was to assess the feasibility and efficiency of CRISPR/Cas-mediated gene editing in the retina using a viral delivery system that could be adapted for use in a clinical setting in the future. To objectively quantify a phenotypic outcome for in vivo gene editing, we designed sgRNA constructs to disrupt a yellow fluorescent protein (*YFP*) in a transgenic mouse. Accordingly, we report the use of a robust, quantifiable means to explore the efficacy of a CRISPR/Cas system for retinal modification and demonstrate clear proof-of-concept evidence for gene modification in vivo.

Methods

Ethics Approval and Colony Maintenance

Ethics approval for this work was obtained from the Animal Ethics Committee of the University of Tasmania (A14827) and St. Vincent's Hospital (AEC 014/15), in accordance with the requirements of the National Health and Medical Research Council of Australia (Australian Code of Practice for the Care and Use of Animals for Scientific Purposes). We adhered to the ARVO Statement for the Use of Animals in Ophthalmic and Vision Research.

Thy1-YFP transgenic mice [B6.Cg-Tg(Thy1-YFP)16Jrs/J], which express YFP in all retinal ganglion cells (RGCs) as well as amacrine cells and bipolar cells in the retina, were obtained from the Jackson Laboratory (mouse stock no: 003709; Bar Harbor, ME, USA) and bred at the mouse facility of the Menzies Institute for Medical Research (Hobart, Australia).[20] Mice were housed in standard conditions (20°C, 12/12 hour light/dark cycle) with access to food and water ad libitum.

sgRNA Design and Construct Generation

Single guide RNAs targeting the 5′ region of the *YFP* gene were designed using the CRISPR design tool (provided in the public domain, http://crispr.mit.edu/) (Supplementary Table S1).[21] The MM9 mouse assembly was used as the reference genome, and three sgRNAs were selected for subsequent profile testing. Yellow fluorescent protein–overexpressing 3T3-L1 (ATCC CL-173; American Type Culture Collection, Manassas, VA, USA) and HEK293A (catalogue no. R70507; Life Technologies, Mulgrave, VIC, Australia) cell lines were used for indel analysis and in vitro validation, respectively (Fig. 1). Control sgRNA sequence targeting *LacZ* was based on the work by Swiech and colleagues.[22] Single guide RNAs were initially cloned into the pSpCas9(BB)purov2.0 vector (a gift from Feng Zhang; Addgene plasmid no. 62988),[21] and the best performing sgRNAs were subsequently cloned into pX552-mCherry (a gift from Feng Zhang; Addgene plasmid nos. 60957 and 60958).[22] pX552-mCherry was generated by replacing the *GFP* with *mCherry* using *Sal*I and *Bsp*EI restriction sites.

Cell Culture and Transfection

Stable cell lines of HEK293A and mouse 3T3-L1 expressing YFP were generated using pAS2.EYFP.puro lentivirus (RNAiCore; Academia Sinica, Taipei, Taiwan) and selected using puromycin or fluorescence-activated cell sorting (FACS). All media components were purchased from Life Technologies. Cell lines were maintained in Dulbecco's modified Eagle's medium (DMEM) (catalogue no. 11995040) supplemented with 10%

fetal bovine serum (FBS; catalogue no. 26140079), 2 mM L-glutamine (catalogue no. 25030081), and 50 U/mL penicillin-streptomycin (catalogue no. 15070063) and cultured at 37°C with 5% CO_2 incubation. Transfection of CRISPR/Cas constructs was performed using lipofectamine 2000 (catalogue no. 11668027; Life Technologies), with 2.5 μg plasmid per well of six-well plates, according to the manufacturer's instructions. Fluorescence images were visualized and captured with a Nikon Eclipse TE2000 inverted microscope (Nikon, Melville, NY, USA).

Indel Analysis

Genomic DNA was extracted using QIAamp DNA mini kit (catalogue no. 51304; Qiagen, Chadstone, VIC, Australia). Indel analysis was performed with the SURVEYOR assay kit (catalogue no. 706020; Integrated DNA Technologies, Inc., Coralville, IA, USA) using 200 to 400 ng PCR products generated from genomic DNA of transfected cells. SURVEYOR primers flanking the cleavage sites are listed in Supplementary Table S1. Polymerase chain reaction cleaved products were resolved on 1.8% Tris/Borate/EDTA (TBE) agarose gel and visualized using GelRed nucleic acid gel stain (catalogue no. 41003; Biotium, Hayward, CA, USA). To determine the spectrum and frequency of indels induced by the sgRNA selected for in vivo work, 3T3L1-YFP cells were transfected with 1.5 μg of each adeno-associated virus 2 (AAV2) plasmid, pX551 and pX552-mCherry with YFP KO sgRNA2, using Fugene HD (catalogue no. E2311; Promega; Madison, WI, USA) following the manufacturer's protocol. Cells were collected on day 6 and FACS sorted for mCherry-positive cells and genomic DNA extracted using QuickExtract DNA Extraction Solution (catalogue no. QE09050; Epicentre, Madison, WI, USA) following the heating cycle 62°C for 20 minutes, 68°C for 20 minutes, and 98°C for 20 minutes. Polymerase chain reaction product was synthesized using Taq DNA polymerase with ThermoPol buffer (catalogue no. M0267S; New England Biolabs, Ipswich, MA, USA). TOPO TA cloning of the PCR fragment into pCR2.1-TOPO vector was conducted following manufacturer's protocol (catalogue no. 45-0641; Life Technologies). Sanger sequencing was used to identify mutations in the *YFP* fragment using the M13 forward primer (−20) included in the kit.

Virus Production

Recombinant AAV2 viruses were produced in HEK293 cells packaging either pX551, containing SpCas9, or pX552-mCherry with the respective sgRNAs, and pseudoserotyped with the AAV2 capsid (pXX2) as previously outlined.[23] Viral vectors were purified by AAV2pro Purification Kit (catalogue no. 6232; Clontech Laboratories, Inc., Mountain View, CA, USA), and vector genomes were titered by real-time quantitative PCR using the following primer sets: (pX551-F: CCGAAGAGGTCGT GAAGAAG, pX551-R: GCCTTATCCAGTTCGCTCAG, pX552-F: TGTGGAAAGGACGAAACACC, pX552-R: TGGTCCTAAAACC CACTTGC) with the SYBR Green Master Mix (catalogue no. 4309155; Life Technologies).

Intraocular Injection of AAV Vectors

A total of 22 adult mice, aged between 14 and 16 weeks, were randomly allocated to receive YFP-sgRNA or LacZ-sgRNA (n = 11 per group). Mice were anesthetized by intraperitoneal injection of ketamine (60 mg/kg) and xylazine (10 mg/kg). Intravitreal injections were performed using a surgical microscope similar to that previously described.[24] In brief, after making a guide track through the conjunctiva and sclera at the superior temporal hemisphere using a 30-gauge needle, a hand-pulled glass micropipette was inserted into the midvitreal cavity. A total of 1 μL dual-viral suspension (AAV2-SpCas9 3×10^9 vector genomes [vg]/μL with AAV2-LacZ-sgRNA 2.5×10^9 vg/μL or AAV2-YFP-sgRNA 3×10^9 vg/μL) or balanced salt solution was injected into each eye at a rate of 100 nL/s using a UMP3-2 Ultra Micro Pump (World Precision Instruments, Inc., Sarasota, FL, USA). Patency was confirmed following needle removal.

Electrophysiological Assessment and Retinal Morphology

Mice were euthanized 5 weeks after intraocular injection. Immediately prior to terminal anesthesia, electroretinography was used to assess retinal function in six mice treated with SpCas9/YFP-sgRNA and six mice treated with SpCas9/LacZ-sgRNA.

Our methods for electroretinogram recordings have been well described previously.[25–27] In brief, overnight dark adaptation (minimum 12 hours) was performed and all animals were prepared for recording under dim red illumination. Following general anesthesia (ketamine 80 mg/kg, xylazine 10 mg/kg), pupil dilation and corneal anesthesia were obtained with 0.5% tropicamide and 0.5% proxymetacaine, respectively. A Ganzfeld sphere (Photometric Solutions International, Oakleigh, VIC, Australia) was used to deliver luminous energy ranging from −6.26 to 2.07 log cd·m^{-2}·s calibrated with an IL1700 integrating photometer (International Light Technologies, Peabody, MA, USA). Electrical signals were recorded with a chlorided silver electrode on the corneal apex and referenced to a ring electrode placed on the conjunctiva posterior to the limbus. A ground needle electrode was placed in the tail. Full-field flash electroretinograms were recorded using standard settings. Response amplitudes of the scotopic a-wave, scotopic b-wave, scotopic threshold response (STR), photopic negative response, and photopic b-wave were measured. Signals were amplified (×1000) over a band pass of 0.3 to 1000 Hz (−3 dB) and digitized using an acquisition rate of 4 kHz. Ganglion cell response was measured as the peak-to-trough amplitude of the STR recorded at −5.25 log cd·m^{-2}·s.[25–27]

Retinal morphology was assessed in vivo using spectral-domain optical coherence tomography (OCT; Bioptigen, Morrisville, NC, USA). Immediately following ERG recordings, a 1.4-mm-wide horizontal B-scan (consisting of 1000 A-scans) of the retina centered at the optic nerve head was obtained. Total retinal thickness (inner retinal surface to retinal pigment epithelium), retinal nerve fiber layer (RNFL; inner retinal surface to nerve fiber layer), and ganglion cell complex (GCC) thickness (inner retinal surface to inner plexiform layer) were returned after manually segmenting key retinal layers (in a masked fashion) followed by averaging thicknesses across a region of interest of 200 to 400 μm from center of the optic nerve. Values from both nasal and temporal retina were averaged.

Retinal Tissue Processing

Enucleated eyes were fixed in 4% paraformaldehyde (PFA; catalogue no. C004; ProSciTech, Townsville City, QLD, Australia) for 1 hour, and retinal flat mounts were prepared and stained with a 4′,6-diamidino-2-phenylindole (DAPI; 0.2 ug/mL; catalogue no. D9542; Sigma-Aldrich; Sydney, NSW, Australia) counterstain. For histologic assessment, enucleated eyes were fixed in 4% PFA for 1 hour and embedded in optimal cutting temperature compound prior to frozen sectioning on a microtome cryostat. Serial 10-μm-thick sections were cut, mounted on silanated glass slides, and then stained with DAPI.

Retinal Imaging, Cell Counting, and Statistical Analysis

A fluorescence microscope (Zeiss Axio Imager Microscope; Carl-Zeiss-Strasse, Oberkochen, Germany) equipped with a charge-coupled device digital camera (Axiocam MRm, Zeiss) and image acquisition software (ZEN2, Zeiss) was used. Following whole mounting, each retinal quadrant was photographed using an appropriate filter for the fluorescence emission spectra of mCherry (605 nm, Zeiss Filter set 64HE) and YFP (495 nm, Zeiss Filter set 38HE). Confocal images were taken using a Nikon C1 confocal laser scanning microscope using a ×20 0.75 NA lens, and images were tile stitched using the NIS Elements AR program. Retinal cell quantification was performed using individual fluorescent images captured at ×400 magnification. A total of 18 images from four flat-mounted eyes treated with SpCas9/LacZ-sgRNA, as well as 26 images from five flat-mounted eyes treated with SpCas9/YFP-sgRNA, were quantified manually using ImageJ v1.49 by an experienced grader (FL), masked to treatment status.[28] To investigate retinal cellular subpopulations targeted by our AAV2 vectors, five retinal cross sections from five SpCas9/LacZ-sgRNA–treated eyes and five retinal cross sections from SpCas9/YFP-sgRNA–treated eyes were also quantified (at ×200 magnification). Sample group decoding was performed only once data were quantified and analyzed.

The efficiency of YFP knockout was determined by the proportion of YFP-negative cells among mCherry-expressing cells. Specifically, the mean proportion of YFP knockout for all eyes treated with SpCas9/YFP-sgRNA was calculated by $\Delta YFP^{-ve}/(\Delta YFP^{-ve} + YFP^{+ve})$, where ΔYFP^{-ve} was the number of mCherry transfected cells in SpCas9/YFP-sgRNA–treated eyes, which did not express YFP, minus the average number of mCherry-expressing cells in SpCas9/LacZ-sgRNA–treated eyes, which did not express YFP (YFP^{-ve}); YFP^{+ve} was the number of cells that expressed both YFP and mCherry.

To profile the putative in vivo activity of the promoters used to drive SpCas9 and mCherry expression in our plasmids, we interrogated the single-cell mouse retinal expression data generated by Macosko et al.[29] (GSE63472). In brief, transcriptomic data from 44,808 retinal cells collected from P14 C57BL/6 mice were analyzed. Hierarchical clustering was used to separate cells into distinct clusters (RGCs, amacrine cells, rods, and so on), and the percentage of cells in each cluster that expressed Mecp1 and Syn1 (i.e., a transcripts per million [TPM] value ≥ 1) was quantified. The mean value from clusters of the same cell type were merged.

Comparisons between continuous traits were made using the paired *t*-test, while categorical data were analyzed using the χ^2 or Fisher exact test. Unless otherwise specified, data are presented as mean ± SD. A total of 14 images were processed twice to determine intragrader variability. The intraclass correlation coefficient for YFP^{+ve} cell counts was 0.945 (95% confidence interval [CI]: 0.842–0.982) and for YFP^{-ve} cell counts was 0.954 (95% CI: 0.867–0.985). Analyses were performed in the R statistical environment (version 3.2.2; in the public domain: https://cran.r-project.org/).

Results

sgRNA Selection and In Vitro Validation

We assessed three sgRNAs targeting the *YFP* sequence, together with a LacZ-sgRNA control,[22] for cleavage efficiency in 3T3-L1-YFP cells (Fig. 1A). Indel analysis for the quantification of sgRNA-induced nucleotide mismatches revealed that one of our sgRNAs (designated YFP KO sgRNA2) targeted *YFP* most effectively (Fig. 1B). Following TOPO TA cloning we found approximately 73% cleavage activity of this YFP-sgRNA, which was then used for all subsequent experiments (Fig. 1D). When transfected into HEK293A-YFP cells, our selected YFP-sgRNA resulted in almost complete reduction in yellow fluorescence compared with untransfected and LacZ-sgRNA controls (Fig. 1C).

In Vivo AAV Delivery and Gene Targeting of CRISPR/Cas9 in the Mouse Retina

To evaluate the YFP disruption in vivo by CRISPR/Cas-mediated gene editing, Thy1-YFP mice received a single intravitreal injection of our dual-viral suspension of AAV2-SpCas9 and AAV2-sgRNA-mCherry (Fig. 2A). In the murine retina, the promoters used for each plasmid (Mecp2 and Syn1 for SpCas9 and mCherry, respectively) have the greatest expression in RGCs and amacrine cells (Supplementary Fig. S1). Five weeks following treatment, inspection of retinal whole-mount images, captured under a stereomicroscope, revealed a lower number of YFP-positive cells from SpCas9/YFP-sgRNA–treated eyes compared to SpCas9/LacZ-sgRNA–treated (Fig. 2) or contralateral control eyes. To quantify the efficiency of YFP disruption following AAV2 delivery of SpCas9 and sgRNA, high-magnification flat-mount images were obtained, and the proportion of YFP-positive and -negative mCherry-expressing cells was calculated. A marked decrease in the number of YFP-positive cells in the inner retina was found in SpCas9/YFP-sgRNA–treated eyes compared to SpCas9/LacZ-sgRNA–treated eyes. The proportion of YFP/mCherry-expressing cells in eyes treated with SpCas9/YFP-sgRNA was 0.106 ± 0.022 compared to SpCas9/LacZ-sgRNA–treated eyes, where the proportion of YFP/mCherry-expressing cells was 0.664 ± 0.050 (Fig. 2D). Overall there was an 84.0% (95% CI: 81.8–86.9) reduction of YFP-positive cells in SpCas9/YFP-sgRNA transfected retinal cells compared to eyes treated with SpCas9/LacZ-sgRNA. As expected, there was no significant variation in the number of YFP cells in untreated control eyes of both groups. Similarly, retinal cross sections showed a clear disruption of YFP expression in the ganglion cell layer (GCL) of the SpCas9/YFP-sgRNA–treated eyes, but not SpCas9/LacZ-sgRNA–treated eyes (Figs. 2F, 2H). Adeno-associated virus 2 was found to predominate in the GCL, with approximately a 50% reduction of YFP-expressing RGCs (Supplementary Fig. S1).

Electroretinography Assessment of Retinal Function

Electrophysiological assessment of mice 5 weeks after treatment with SpCas9/YFP-sgRNA or SpCas9/LacZ-sgRNA confirmed no adverse effects on photoreceptoral (a-wave: YFP $P = 0.64$; LacZ $P = 0.35$) or bipolar cell (b-wave: YFP $P = 0.38$; LacZ $P = 0.40$) function (Fig. 3; Supplementary Figs. S2–S4). Importantly, given the AAV2 transfection profile following intravitreal injection, inner retinal function as indicated by the oscillatory potentials (YFP $P = 0.42$; lacZ $P = 0.68$) was also not disrupted (Fig. 3; Supplementary Fig. S2). The amplitude, indicative of ganglion cell activity, did not significantly differ between YFP-sgRNA–treated and contralateral control eyes ($P = 0.48$), or between LacZ-sgRNA–treated and their contralateral eyes ($P = 0.87$) (Supplementary Fig. S4).

There was no statistically significant difference in retinal morphologic profiles in situ between treated and contralateral control eyes (Supplementary Fig. S5). In particular, the RNFL and GCC thickness as measured by OCT did not significantly differ between eyes treated with YFP-sgRNA and contralateral control eyes (RNFL $P = 0.30$, GCC $P = 0.80$) or between LacZ-sgRNA and their control eyes (RNFL $P = 0.70$, GCC $P = 0.39$).

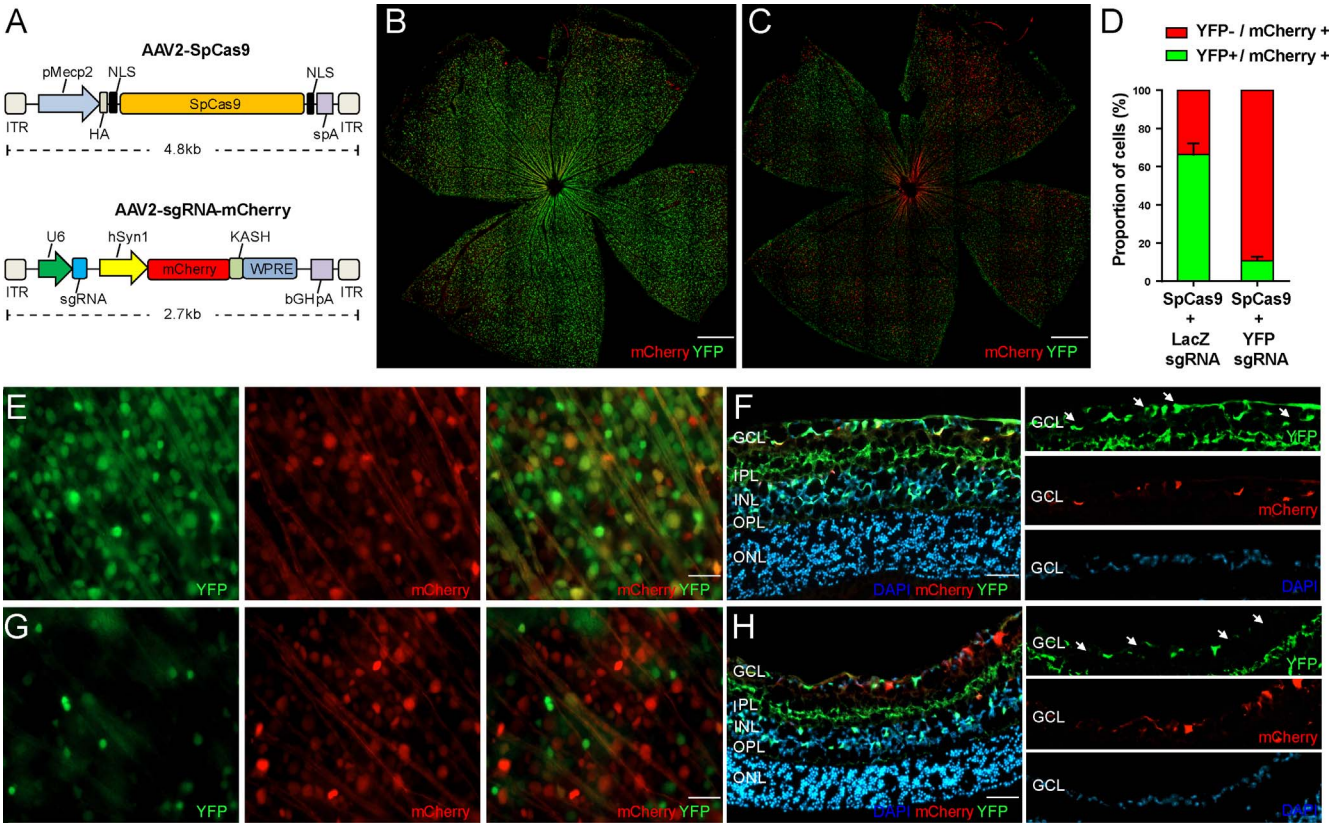

Figure 2. CRISPR/Cas-mediated gene editing of retinal cells in vivo. Dual-viral suspension of AAV2-SpCas9 and AAV2-sgRNA was used (**A**). sgRNA plasmids also expressed mCherry, and the size of the cassettes packaged by AAV2 is displayed. Representative retinal montages from Thy1-yellow fluorescent protein (YFP) mice exposed in vivo to our dual AAV2 plasmid system carrying SpCas9 and either control (LacZ) sgRNA (**B**) or sgRNAs targeting YFP (**C**) (*scale bar*: 500 μm). Overall, the proportion of mCherry-expressing cells (mCherry+), which lacked YFP (YFP–), was higher in SpCas9/YFP-sgRNA–treated eyes (**D**). Higher magnification of flat-mount images, displaying differences in YFP expression following AAV2-mediated delivery of SpCas9/LacZ-sgRNA (**E**) or SpCas9/YFP-sgRNA (**G**) (*scale bar*: 10 μm). Cross sections displaying AAV2 infection of the inner retina confirm YFP knockout in SpCas9/YFP-sgRNA–treated eyes (**H**), compared to SpCas9/LacZ-sgRNA–treated eyes (**F**) (*scale bar*: 50 μm). *White arrows* indicate AAV2-sgRNA–infected cells. Abbreviations: GCL, ganglion cell layer; IPL, inner plexiform layer; INL, inner nuclear layer; OPL, outer plexiform layer; ONL, outer nuclear layer; ITR; inverted terminal repeat; pMecp2, truncated methyl-CpG-binding protein 2 promoter; HA, hemagglutinin tag; NLS, nuclear localization signal; spA, synthetic polyadenylation signal; U6, Pol III promoter; sgRNA, single guide RNA; hSyn1, human synapsin 1 promoter; mCherry, monomeric cherry fluorescent protein; KASH, Klarsicht ANC1 Syne homology nuclear transmembrane domain; WPRE, woodchuck hepatitis virus posttranscriptional regulatory element; bGHpA, bovine growth hormone polyadenylation signal.

Discussion

We have successfully demonstrated viral-mediated delivery of essential CRISPR/Cas components to retinal cells in vivo. Using a transgenic fluorescent mouse model, we have definitive evidence for CRISPR/Cas-mediated gene editing of *Thy1*-expressing retinal cells. With our dual-viral SpCas9/sgRNA suspension we observed a reduction of YFP-positive cells of approximately 84.0% (95% CI: 81.8–86.9). This level of gene modulation in vivo is similar to that reported for other tissues, such as brain (~68% using AAV) and liver (80–90% using adenovirus).[22,30]

Our study builds on recent work in which the CRISPR/Cas system was introduced into rodent retinas using an electroporation delivery method.[18,19] By demonstrating that CRISPR/Cas can also cause substantial gene modification activity when introduced by a viral delivery method in the retina, we are closer to translating gene editing technology for therapeutic purposes. Importantly, we found that AAV2-delivered SpCas9 was not retinotoxic over a 5-week treatment period. Nonetheless, it is clearly possible that adverse effects from ongoing or prolonged CRISPR/Cas expression could arise. As such it will be important to continue to develop CRISPR/Cas systems that could be tightly regulated and thereby be able to create an optimal window for gene modification while reducing the chance for potential off-target activity.[31–34]

Adeno-associated viral vectors have been widely exploited as a promising tool for gene delivery in vivo, and it is clear that combining alternate AAVs and sgRNA promoters will extend the CRISPR/Cas therapeutic repertoire. Specifically, different AAV serotypes have the ability to transfect distinct cell populations within the retina,[35] and while the AAV2 capsid used in our study is known to primarily transduce RGCs when injected intravitreally,[36] a different AAV2 variant, 7m8, can infect photoreceptors following intravitreal delivery.[37] Additionally, to overcome the packaging size limitation of AAV vectors,[38] we used a dual-vector system to package SpCas9 and sgRNA expression cassettes in two separate viral vectors. Although a single vector that packages a smaller Cas9 orthologue, such as *Staphylococcus aureus* Cas9 (SaCas9), together with a sgRNA, could achieve greater knockout efficiencies in vivo,[17,39,40] dual-vector systems may still be required for mutation correction by enabling the cellular delivery of additional donor templates and appropriate promoter elements. For example, a recent study from Yang and colleagues[41] demonstrated that a two-vector approach with SaCas9 resulted in mutation correction in approximately 10% of hepatocytes in ornithine transcarbamylase–deficient newborn mice. With ongoing advances in viral

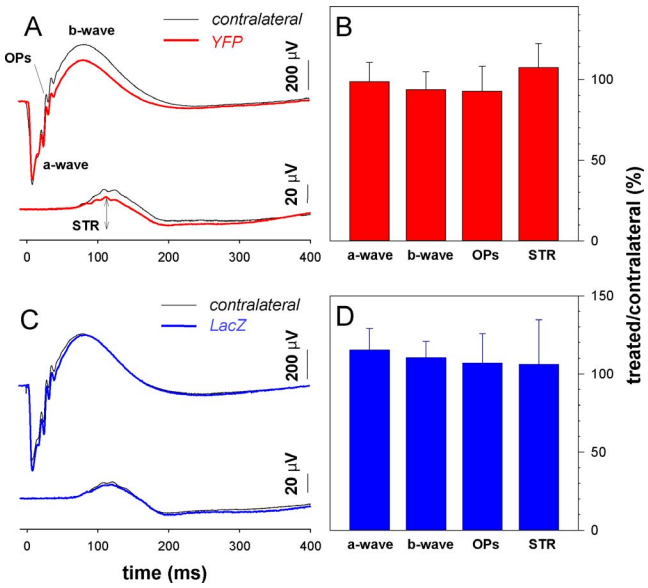

FIGURE 3. Effect of SpCas9 on retinal function. Averaged ERG waveforms at selected intensities for YFP-sgRNA–treated ($n = 6$, *red*) and contralateral ($n = 6$, *black*) eyes (**A**). The average photoreceptoral (a-wave), bipolar cell (b-wave), amacrine cell (oscillatory potentials, OPs), and ganglion cell (scotopic threshold response, STR) amplitude in YFP-sgRNA–treated relative to contralateral control eyes (%, ±SEM) is displayed (**B**). (**C**) The averaged ERG waveforms at selected intensities in LacZ-sgRNA–treated ($n = 6$, *blue*) and contralateral eyes ($n = 6$, *black*). The LacZ-sgRNA group's average a-wave, b-wave, OPs, and STR amplitude relative to contralateral control eyes (%, ±SEM) (**D**).

engineering and the development of new serotypes, future research investigating the efficacy of different viral-CRISPR/Cas systems in the retina is warranted.

An important limitation of our work is the fact that off-target effects were not directly quantified. Nonetheless, to some extent this is a minor consideration for our initial proof-of-concept work, which sought to primarily assess "on-target" efficacy of virally delivered CRISPR/Cas in the adult retina. Additionally, it is well appreciated that CRISPR/Cas technology is advancing rapidly, and although a major limitation of gene editing has been the prospect of off-target effects, this issue is being addressed.[33,34] For example, with careful design of the guide RNA (using a double nick; truncated sgRNA), it is already possible to avoid most off-target cuts; and recently, two independent studies reported modifications to SpCas9, which can dramatically reduce off-target activity.[33,34] In any case, it is clear that safety will be paramount prior to the use of CRISPR/Cas in mainstream medical care, and off-target profiling will need to be considered before current research is translated into clinical trials.

In summary, this work suggests that a relatively high efficiency of gene editing in the retina can be achieved by a dual AAV2-mediated CRISPR/Cas system. While ex vivo transcription activator-like effector nucleases (TALEN)-based approaches are now in clinical trials, given the versatility and relative ease of design, CRISPR/Cas techniques appear to be more clinically applicable. Inherited eye diseases share several features that make them appealing for the application of in vivo gene editing. For example, nonsyndromic retinal diseases generally have a specific and well-defined pathogenesis, such that only a specific subpopulation of cells would need to be targeted. Additionally, following any intervention, the eye can be directly examined for the development of any adverse effects. Nonetheless, any in vivo gene editing therapies will require a number of functionally active cells, and it is possible that the threshold for viable cells will vary across genes and diseases.

Acknowledgments

We thank Kenneth Pang, Sze Woei Ng, Elsa Chan, Stacey Jackson, Zheng He, and Olivia Swann.

Supported by grants from the BrightFocus Foundation, the Ophthalmic Research Institute of Australia, Retina Australia, the Childhood Eye Cancer Trust, and the Eye Research Australia Fund. AP and BVB are supported by Australian Research Council Future Fellowships. AWH is supported by a National Health and Medical Research Council Practitioner Fellowship. Centre for Eye Research Australia (CERA) receives operational infrastructure support from the Victorian Government.

Disclosure: **S.S.C. Hung**, None; **V. Chrysostomou**, None; **F. Li**, None; **J.K.H. Lim**, None; **J.-H. Wang**, None; **J.E. Powell**, None; **L. Tu**, None; **M. Daniszewski**, None; **C. Lo**, None; **R.C. Wong**, None; **J.G. Crowston**, None; **A. Pébay**, None; **A.E. King**, None; **B.V. Bui**, None; **G.-S. Liu**, None; **A.W. Hewitt**, None

References

1. Liew G, Michaelides M, Bunce C. A comparison of the causes of blindness certifications in England and Wales in working age adults (16-64 years), 1999-2000 with 2009-2010. *BMJ Open*. 2014;4:e004015.
2. Chiang JP, Trzupek K. The current status of molecular diagnosis of inherited retinal dystrophies. *Curr Opin Ophthalmol*. 2015;26:346–351.
3. Hartong DT, Berson EL, Dryja TP. Retinitis pigmentosa. *Lancet*. 2006;368:1795–1809.
4. den Hollander AI. Omics in ophthalmology: advances in genomics and precision medicine for Leber congenital amaurosis and age-related macular degeneration. *Invest Ophthalmol Vis Sci*. 2016;57:1378–1387.
5. Tucker BA, Mullins RF, Stone EM. Stem cells for investigation and treatment of inherited retinal disease. *Hum Mol Genet*. 2014;23:R9–R16.
6. Bainbridge JW, Mehat MS, Sundaram V, et al. Long-term effect of gene therapy on Leber's congenital amaurosis. *N Engl J Med*. 2015;372:1887–1897.
7. Jacobson SG, Cideciyan AV, Roman AJ, et al. Improvement and decline in vision with gene therapy in childhood blindness. *N Engl J Med*. 2015;372:1920–1926.
8. Trapani I, Toriello E, de Simone S, et al. Improved dual AAV vectors with reduced expression of truncated proteins are safe and effective in the retina of a mouse model of Stargardt disease. *Hum Mol Genet*. 2015;24:6811–6825.
9. Thompson DA, Ali RR, Banin E, et al. Advancing therapeutic strategies for inherited retinal degeneration: recommendations from the Monaciano Symposium. *Invest Ophthalmol Vis Sci*. 2015;56:918–931.
10. Daiger SP, Bowne SJ, Sullivan LS. Genes and mutations causing autosomal dominant retinitis pigmentosa. *Cold Spring Harb Perspect Med*. 2014;5i:a017129.
11. Mali P, Yang L, Esvelt KM, et al. RNA-guided human genome engineering via Cas9. *Science*. 2013;339:823–826.
12. Cong L, Ran FA, Cox D, et al. Multiplex genome engineering using CRISPR/Cas systems. *Science*. 2013;339:819–823.
13. Cox DB, Platt RJ, Zhang F. Therapeutic genome editing: prospects and challenges. *Nat Med*. 2015;21:121–131.
14. Yin H, Xue W, Chen S, et al. Genome editing with Cas9 in adult mice corrects a disease mutation and phenotype. *Nat Biotechnol*. 2014;32:551–553.

15. Long C, Amoasii L, Mireault AA, et al. Postnatal genome editing partially restores dystrophin expression in a mouse model of muscular dystrophy. *Science*. 2016;351:400–403.
16. Nelson CE, Hakim CH, Ousterout DG, et al. In vivo genome editing improves muscle function in a mouse model of Duchenne muscular dystrophy. *Science*. 2016;351:403–407.
17. Tabebordbar M, Zhu K, Cheng JK, et al. In vivo gene editing in dystrophic mouse muscle and muscle stem cells. *Science*. 2016;351:407–411.
18. Wang S, Sengel C, Emerson MM, et al. A gene regulatory network controls the binary fate decision of rod and bipolar cells in the vertebrate retina. *Dev Cell*. 2014;30:513–527.
19. Bakondi B, Lv W, Lu B, et al. In vivo CRISPR/Cas9 gene editing corrects retinal dystrophy in the S334ter-3 rat model of autosomal dominant retinitis pigmentosa. *Mol Ther*. 2016;24:556–563.
20. Feng G, Mellor RH, Bernstein M, et al. Imaging neuronal subsets in transgenic mice expressing multiple spectral variants of GFP. *Neuron*. 2000;28:41–51.
21. Ran FA, Hsu PD, Wright J, et al. Genome engineering using the CRISPR-Cas9 system. *Nat Protoc*. 2013;8:2281–2308.
22. Swiech L, Heidenreich M, Banerjee A, et al. In vivo interrogation of gene function in the mammalian brain using CRISPR-Cas9. *Nat Biotechnol*. 2015;33:102–106.
23. Xiao X, Li J, Samulski RJ. Production of high-titer recombinant adeno-associated virus vectors in the absence of helper adenovirus. *J Virol*. 1998;72:2224–2232.
24. Grant CA, Ponnazhagan S, Wang XS, et al. Evaluation of recombinant adeno-associated virus as a gene transfer vector for the retina. *Curr Eye Res*. 1997;16:949–956.
25. Kohzaki K, Vingrys AJ, Bui BV. Early inner retinal dysfunction in streptozotocin-induced diabetic rats. *Invest Ophthalmol Vis Sci*. 2008;49:3595–3604.
26. Nguyen CT, Vingrys AJ, Wong VH, et al. Identifying cell class specific losses from serially generated electroretinogram components. *Biomed Res Int*. 2013;2013:796362.
27. Crowston JG, Kong YX, Trounce IA, et al. An acute intraocular pressure challenge to assess retinal ganglion cell injury and recovery in the mouse. *Exp Eye Res*. 2015;141:3–8.
28. Schneider CA, Rasband WS, Eliceiri KW. NIH Image to ImageJ: 25 years of image analysis. *Nat Methods*. 2012;9:671–675.
29. Macosko EZ, Basu A, Satija R, et al. Highly parallel genome-wide expression profiling of individual cells using nanoliter droplets. *Cell*. 2015;161:1202–1214.
30. Cheng R, Peng J, Yan Y, et al. Efficient gene editing in adult mouse livers via adenoviral delivery of CRISPR/Cas9. *FEBS Lett*. 2014;588:3954–3958.
31. Zuris JA, Thompson DB, Shu Y, et al. Cationic lipid-mediated delivery of proteins enables efficient protein-based genome editing in vitro and in vivo. *Nat Biotechnol*. 2015;33:73–80.
32. Dow LE, Fisher J, O'Rourke KP, et al. Inducible in vivo genome editing with CRISPR-Cas9. *Nat Biotechnol*. 2015;33:390–394.
33. Slaymaker IM, Gao L, Zetsche B, et al. Rationally engineered Cas9 nucleases with improved specificity. *Science*. 2016;351:84–88.
34. Kleinstiver BP, Pattanayak V, Prew MS, et al. High-fidelity CRISPR-Cas9 nucleases with no detectable genome-wide off-target effects. *Nature*. 2016;529:490–495.
35. Dalkara D, Kolstad KD, Caporale N, et al. Inner limiting membrane barriers to AAV-mediated retinal transduction from the vitreous. *Mol Ther*. 2009;17:2096–2102.
36. Vandenberghe LH, Auricchio A. Novel adeno-associated viral vectors for retinal gene therapy. *Gene Ther*. 2012;19:162–168.
37. Dalkara D, Byrne LC, Klimczak RR, et al. In vivo-directed evolution of a new adeno-associated virus for therapeutic outer retinal gene delivery from the vitreous. *Sci Transl Med*. 2013;5:89ra76.
38. Wu Z, Yang H, Colosi P. Effect of genome size on AAV vector packaging. *Mol Ther*. 2010;18:80–86.
39. Ran FA, Cong L, Yan WX, et al. In vivo genome editing using Staphylococcus aureus Cas9. *Nature*. 2015;520:186–191.
40. Friedland AE, Baral R, Singhal P, et al. Characterization of Staphylococcus aureus Cas9: a smaller Cas9 for all-in-one adeno-associated virus delivery and paired nickase applications. *Genome Biol*. 2015;16:257.
41. Yang Y, Wang L, Bell P, et al. A dual AAV system enables the Cas9-mediated correction of a metabolic liver disease in newborn mice. *Nat Biotechnol*. 2016;34:334–338.

Investigative Ophthalmology & Visual Science